

# The Halo White Dwarf WD 0346+246 Revisited

P. Bergeron

*Département de Physique, Université de Montréal, C.P. 6128, Succ. Centre-Ville, Montréal,  
Québec, Canada, H3C 3J7.*

bergeron@astro.umontreal.ca

## ABSTRACT

The extreme helium-rich atmospheric composition determined for the halo white dwarf WD 0346+246 is reexamined. This solution is shown to be improbable from an astrophysical point of view when accretion of hydrogen and metals from the interstellar medium is taken into account. An alternate solution is proposed where hydrogen and helium are present in the atmospheric regions in equal amounts. The best fit at  $T_{\text{eff}} = 3780$  K,  $\log g = 8.34$ , and  $N(\text{He})/N(\text{H}) = 1.3$  is achieved by including in the model calculations a bound-free opacity from the Lyman edge associated with the so-called dissolved atomic levels of the hydrogen atom, or pseudo-continuum opacity.

*Subject headings:* stars: atmospheres — atomic processes — stars: individual (WD 0346+246) — white dwarfs

## 1. Introduction

The luminosity function of cool white dwarfs determined from proper motion surveys (Liebert et al. 1988; Monet et al. 1992) or colorimetric surveys (Knox et al. 1999) exhibits a sharp peak near  $\log L/L_{\odot} = -4.1$ , followed by a sudden drop towards lower luminosities. The paucity of white dwarfs at low luminosities ( $\log L/L_{\odot} \sim -4.4$ ) has been interpreted as a natural consequence of the finite age of the local Galactic disk. These luminosity functions can be combined with theoretical cooling sequences to derive an upper limit of 11 Gyr for the age of the local disk (see the review of Fontaine et al. 2001). Analyses of the coolest objects in these surveys have revealed no evidence for white dwarfs cooler than  $T_{\text{eff}} \sim 4000$  K (Bergeron et al. 1997; Knox et al. 1999; Bergeron et al. 2001).

A handful of cooler and thus older white dwarfs, most likely belonging to the thick disk or halo population, has recently been identified (Hambly et al. 1999; Harris et al. 1999; Ibata et al. 2000; Harris et al. 2001; Oppenheimer et al. 2001b). This small sample has been substantially increased by the exciting discovery by Oppenheimer et al. (2001a) of 38 cool halo white dwarf candidates in the SuperCOSMOS Sky Survey, although the halo nature of these objects has recently been challenged by Reid et al. (2001). The energy distributions of the coolest white dwarfs in these samples are

characterized by a strong infrared flux deficiency and blue optical colors which have been interpreted as the result of extremely strong collision-induced absorptions by molecular hydrogen (Hansen 1998; Saumon & Jacobson 1999).

Although the discovery of such faint and bluish white dwarfs confirms the qualitative trends expected from model atmosphere calculations, quantitative analyses of these objects have been less than successful, in contrast to the detailed analyses of hotter ( $T_{\text{eff}} \gtrsim 4000$  K) white dwarfs in the Galactic disk (Bergeron et al. 1997, 2001). For instance, the energy distributions of LHS 3250 and its almost identical twin SDSS 1337+00 show a maximum peak that is considerably broader and bluer than predicted from pure hydrogen model atmospheres (Harris et al. 1999, 2001). The discrepancy between the models and the observations has been attributed to some missing opacity, most likely originating from collision-induced absorptions by molecular hydrogen due to collisions with *neutral helium*, although this interpretation could not be confirmed quantitatively (Harris et al. 1999; Oppenheimer et al. 2001b). The temperature and composition of these two white dwarfs thus remain unknown.

Oppenheimer et al. (2001b) provided a detailed analysis of the halo white dwarf WD 0346+246, as well as a preliminary analysis of F351–50, discovered respectively by Hambly et al. (1997) and Ibata et al. (2000). For WD 0346+246, Oppenheimer et al. obtained an excellent fit to the observed optical *UBVRI* and infrared *JHK* photometry (see their Fig. 8). Their solution suggests a cool ( $T_{\text{eff}} = 3750$  K) and helium-rich atmospheric composition, with an extremely small hydrogen abundance of  $\log N(\text{H})/N(\text{He}) = -6.4$ .

In this paper, we reexamine the solution proposed by Oppenheimer et al. for WD 0346+246, and demonstrate from simple astrophysical considerations that such a low hydrogen abundance is very unlikely. We first review in § 2 the importance of collision-induced opacities in cool white dwarfs, and discuss the improvements to our model atmosphere grid in § 3. The low hydrogen abundance solution for WD 0346+246 is then critically reevaluated in § 4. A modified treatment of the pseudo-continuum opacity from the Lyman edge is introduced in § 5, while our alternate solution using this previously neglected source of opacity is discussed at length in § 6. Our conclusions follow in § 7.

## 2. Collision-Induced Absorptions by $\text{H}_2$ in Cool White Dwarfs

The energy distributions of cool white dwarfs are characterized by a strong infrared flux deficiency resulting from collision-induced absorptions by molecular hydrogen ( $\text{H}_2$  CIA). Hansen (1998) has recently demonstrated that the location of objects blueward of the white dwarf cooling sequence in the  $M_V$  vs  $(V - I)$  color-magnitude diagram is actually the result of  $\text{H}_2$  CIA which extends well into the optical regions of the energy distribution of cool ( $T_{\text{eff}} \lesssim 3000$  K) and old ( $\tau \gtrsim 11$  Gyr) hydrogen atmosphere white dwarfs (see also Saumon & Jacobson 1999; Bergeron et al. 2001). White dwarf stars thus become increasingly redder as they cool down to  $T_{\text{eff}} \sim 4000$  K, after which they

evolve into bluer objects again. Recent papers reporting the discovery of extremely cool white dwarfs have perpetuated what has now become a common belief that the CIA opacity is important only in this temperature range, however. It thus seems appropriate here to first review our current knowledge of the importance of H<sub>2</sub> CIA in cool white dwarf atmospheres.

In pure hydrogen atmospheres, the H<sub>2</sub> collision-induced opacity is mainly due to collisions with other hydrogen molecules (H<sub>2</sub>-H<sub>2</sub> CIA). This absorption process becomes an important source of infrared opacity in white dwarfs cooler than  $T_{\text{eff}} \sim 5000$  K (see Fig. 5 of Bergeron et al. 1995). At  $T_{\text{eff}} = 4000$  K, for instance, more than 50% of the flux at 2 microns is absorbed by molecular hydrogen. It is only below  $\sim 4000$  K, however, that the H<sub>2</sub> CIA opacity starts affecting the *optical regions* of the energy distribution. Hence, optical color indices of extremely cool white dwarfs, such as  $(V - I)$ , become smaller (i.e., the objects become bluer), as first pointed out by Hansen (1998). Color indices in the infrared, however, become affected at much higher effective temperatures, as shown in the  $(B - V, V - K)$  diagram of Bergeron et al. (1997, their Fig. 9).

Cool white dwarfs with mixed hydrogen and helium abundances are characterized by even stronger infrared flux deficiencies. The absorption by molecular hydrogen in this case is due to collisions with both H<sub>2</sub> and neutral helium (H<sub>2</sub>-He CIA). In white dwarf atmospheres where helium is the dominant constituent, H<sub>2</sub>-He CIA may even represent the dominant source of opacity in the infrared (see Fig. 6 of Bergeron et al. 1995). Even though the H<sub>2</sub>-H<sub>2</sub> and H<sub>2</sub>-He CIA absorption coefficients are extremely similar (see Fig. 7 of Jørgensen et al. 2000), the atmospheric pressures of mixed helium/hydrogen atmospheres are considerably larger than those found in pure hydrogen atmospheres, and as such, the collision-induced absorptions are correspondingly more important. Consequently, the color-indices of mixed composition atmospheres become affected by collision-induced absorptions at much higher effective temperatures than those of pure hydrogen atmospheres, as illustrated in the  $(B - V, V - K)$  two-color diagram shown in Bergeron et al. (1997, Fig. 9). Cool white dwarfs with mixed compositions thus easily stand out in such diagrams. LHS 1126 represents the first white dwarf successfully interpreted in terms of H<sub>2</sub>-He CIA in a mixed hydrogen/helium atmosphere (Bergeron et al. 1994); it is important to point out in this context that the case of LHS 1126 is a definite confirmation of the presence of H<sub>2</sub>-He CIA in a cool white dwarf, and not a *possible* identification, as suggested by Harris et al. (1999).

### 3. Model Atmospheres

Bergeron et al. (1995) calculated model atmospheres with mixed hydrogen and helium abundances of  $N(\text{He})/N(\text{H}) = 0.1, 1, \text{ and } 10$ . Theoretical colors calculated from these models indicate that when the helium abundance is increased, the photometric sequences further deviate from the pure hydrogen sequence *as well as from the pure helium sequence*, as a result of increased collision-induced absorptions. As first pointed out by Bergeron et al. (1995), the photometric sequences of models with even larger helium abundances must at some point move back towards the pure helium sequence. Cool model atmospheres with  $N(\text{H})/N(\text{He}) \lesssim 10^{-3}$  could not be calculated at that time,

however, since the photospheric pressure that characterizes such low hydrogen abundance atmospheres is so high that the hydrogen atomic levels — including that of the  $\text{H}^-$  ion — are strongly perturbed, and must be treated carefully within the occupation probability formalism of Hummer & Mihalas (1988), which had not been included in these earlier models (see § 5.3 of Bergeron et al. 1997).

Details of our current model grid are discussed in Bergeron et al. (2001) and references therein. In particular, the Hummer-Mihalas formalism has now been included in detail following the work of Malo et al. (1999). This improvement now allows us to calculate cool white dwarf models with arbitrarily low hydrogen abundances. Also, the  $\text{He}_2^+$  ion has been included self-consistently in the ionization equilibrium; as discussed by Malo et al., the  $\text{He}_2^+$  ion may completely govern the electron density in cool ( $T_{\text{eff}} \lesssim 8500$  K) helium-rich models. For the purpose of this study, we also make use of the recent *ab initio*  $\text{H}_2$ -He CIA calculations presented in Jørgensen et al. (2000). Earlier white dwarf models used by Bergeron et al. (1997, 2001), and those calculated by Oppenheimer et al. (2001b), all relied on approximate calculations that are partially based on the work of Borysow & Frommhold (see Lenzuni et al. 1991, and references therein). The differences between the new calculations and the previous approximations are significant, particularly at low temperatures (see Figs. 1 and 6 of Jørgensen et al. 2000).

Models with extremely low hydrogen abundances,  $N(\text{H})/N(\text{He}) \lesssim 10^{-7}$ , have also been presented in Oppenheimer et al. (2001b) and used to analyze the cool white dwarf WD 0346+246, although no details of the physics used in these models are provided.

The effects of helium abundance variations on the emergent fluxes of a  $T_{\text{eff}} = 3750$  K,  $\log g = 8.0$  white dwarf model — i.e., the effective temperature and surface gravity derived by Oppenheimer et al. (2001b) for WD 0346+246 — are illustrated in Figure 1. Although the model atmosphere grid has been calculated with a resolution of 1 dex in  $\log N(\text{He})/N(\text{H})$ , only representative models are shown here. As expected, the infrared flux deficiency becomes more important as the helium abundance is gradually increased, until it reaches a maximum at  $N(\text{He})/N(\text{H}) = 10^5$ . Simultaneously, the peak of the energy distribution moves towards shorter wavelengths, and the slope of the optical regions becomes steeper (the star appears bluer). When the helium abundance is further increased,  $\text{H}_2$ -He CIA becomes only a small contribution to the total opacity, the infrared depression weakens, and the peak of the energy distribution rapidly shifts towards longer wavelengths. Similar results were obtained by Oppenheimer et al. (2001b) in two-color diagrams (see their Figs. 6 and 7), although the convergence on the pure helium sequence that occurs at  $N(\text{He})/N(\text{H}) \gtrsim 10^{13}$  in our models was not reached in their analysis. Note that the most extreme helium abundance models discussed here do not take into account the nonideal effects included in the equation-of-state of the pure helium model grid calculated by Bergeron et al. (1995), and as such, these models should be considered illustrative only.

#### 4. Reappraisal of the Low Hydrogen Abundance Solution

We now attempt to fit the observed energy distribution of WD 0346+246 using the fitting technique described in Bergeron et al. (2001). Briefly, the optical *BVRI* and infrared *JHK* magnitudes taken from Table 1 of Oppenheimer et al. (2001b) are first converted into average fluxes using equation (1) of Bergeron et al. (1997). These fluxes are then compared, using a nonlinear least-squares method, with those obtained from the model atmospheres, properly averaged over the filter bandpasses. Only  $T_{\text{eff}}$  and the solid angle  $(R/D)^2$  are considered free parameters. The distance  $D$  is obtained from the trigonometric parallax measurement, if available, and the stellar radius  $R$  is converted into mass using C/O-core cooling sequences described in Bergeron et al. (2001) with thin or thick hydrogen layers, which are based on the calculations of Fontaine et al. (2001). For comparisons, however, we first adopt the temperature and surface gravity from Oppenheimer et al. (2001b).

Our best fit is presented in Figure 2. The top panel shows the results in terms of  $\log f_\lambda$ , which is the representation used by Oppenheimer et al. (2001b, see their Fig. 8), while the bottom panel is in terms of  $f_\nu$ , which is the way fits are displayed in Bergeron et al. (1997, 2001). Hence a good fit could be achieved with  $\log N(\text{He})/N(\text{H}) = 9.1$ , which is qualitatively similar to the best fit obtained in Figure 8 of Oppenheimer et al. Our fit could even perhaps be improved by allowing  $T_{\text{eff}}$  and  $\log g$  to vary. We also note that the discrepancy observed for the *I* bandpass in the lower panel of Figure 2 is also present in the solution of Oppenheimer et al., but this discrepancy becomes less apparent when the solution is presented in terms of  $\log f_\lambda$  (upper panel). Both solutions differ quantitatively by nearly 3 orders of magnitude in helium abundance, however. The origin of this difference is unknown, but may stem from the differences in the input physics used in the two model sets. The important aspect of both solutions nevertheless remains that an *extremely high helium abundance is required to fit the observed energy distribution of WD 0346+246*.

Such a low hydrogen content of only  $N(\text{H})/N(\text{He}) \sim 10^{-9}$  is quite unrealistic, however. Indeed, the white dwarf cooling age of WD 0346+246 implied by our atmospheric parameter determination is 9.6 Gyr (using the thick layer evolutionary models described above; thin layer models yield 8.9 Gyr), during which the star has been traveling across the Galaxy, accreting material from the interstellar medium, including large amounts of hydrogen. Even though elements heavier than helium will rapidly sink below the photosphere because of the efficient gravitational chemical separation that exists in white dwarf atmospheres, hydrogen will tend to float to the surface in the absence of competing mechanisms. In other words, *the hydrogen abundance can only increase with time*. Since the superficial layers of cool white dwarfs are strongly convective, however, hydrogen accreted from the interstellar medium will be homogeneously mixed with the helium convective zone. Below  $T_{\text{eff}} \sim 12,000$  K, the mass of this helium convection zone is almost constant at  $M_{\text{He-conv}} \sim 10^{-6} M_*$  (Tassoul et al. 1990). The hydrogen abundance determined here for WD 0346+246 thus implies a total mass of hydrogen accreted of  $1.2 \times 10^{-16} M_\odot$ , and an accretion rate from the interstellar medium of  $1.3 \times 10^{-26} M_\odot \text{ yr}^{-1}$  (or  $6.3 \times 10^{-24} M_\odot \text{ yr}^{-1}$  if we use the abundance value of Oppenheimer et al.). Such low accretion rates are of course completely unrealistic and would re-

quire extremely efficient screening mechanisms. For instance, the theoretical estimates of Wesemael (1979) suggest time-averaged accretion rates of  $\sim 10^{-17} M_{\odot} \text{ yr}^{-1}$ . Similarly, the two-phase accretion model invoked by Dupuis et al. (1993) to account for the presence of metals in cool helium-rich white dwarfs assumes that accretion is most of the time small, typically  $10^{-20} M_{\odot} \text{ yr}^{-1}$ , but may proceed at a much higher rate of  $5 \times 10^{-15} M_{\odot} \text{ yr}^{-1}$  during passages through dense interstellar clouds.

The extreme purity of the atmosphere suggested for WD 0346+246 also represents a problem if the presence of metals is considered. Even though elements heavier than helium will diffuse downward at the bottom of the helium convection zone with time scales much shorter than the evolutionary time scales (see Dupuis et al. 1992, and references therein), magnesium, calcium, and iron lines are nevertheless often observed in the spectra of cool, helium-rich white dwarfs — the so-called DZ stars. The only viable explanation for the presence of these metals is provided by the accretion-diffusion model in which a balance is achieved between the gravitational settling of metals at the base of the helium convection zone and the accretion of these elements at the surface of the star, most of the time through the low-density interstellar medium, but occasionally through denser “clouds” (see, e.g., Dupuis et al. 1993).

Model atmospheres have been calculated by including metals in the equation-of-state only; metallic opacities, which are negligible at the abundances and temperatures considered here, are not taken into account. The main effect of the presence of heavy elements is to provide free electrons, and to increase the contribution of the  $\text{He}^-$  free-free opacity — the dominant opacity source in pure helium models. Here we include only one heavy element, calcium, the most common metal observed in DZ stars. Calcium abundances determined in DZ stars are typically  $N(\text{Ca})/N(\text{He}) = 10^{-11} - 10^{-10}$ , although abundances as high as  $10^{-8}$  have also been observed in some objects (Zeidler-K. T. et al. 1986). Since calcium lines are not observed in the spectrum of WD 0346+246, we consider calcium abundances much lower than those determined in typical DZ stars. The results of our calculations for white dwarf models with  $T_{\text{eff}} = 3750 \text{ K}$ ,  $\log g = 8.0$ ,  $\log N(\text{He})/N(\text{H}) = 9.1$ , and for  $N(\text{Ca})/N(\text{He}) = 0, 10^{-14}, 10^{-13},$  and  $10^{-12}$  are displayed in Figure 3, together with the photometric observations of WD 0346+246 shown for comparison. This experiment shows that even with a low calcium abundance of only  $N(\text{Ca})/N(\text{He}) = 10^{-14}$ , the infrared fluxes are significantly different from those obtained with the zero-metallicity model, and different from the observed fluxes of WD 0346+246 as well. Higher calcium abundances — and the inclusion of additional elements such as magnesium or iron — would probably make matters even worse.

We thus conclude that an almost pure helium atmospheric composition for WD 0346+246, or any cool white dwarf in this temperature range for that matter, represents an unlikely solution. In the following sections, we propose an alternate solution for this object.

## 5. Pseudo-Continuum Opacity from the Lyman Edge

Bergeron et al. (1997) showed that the photometric observations of DA (hydrogen-line) white dwarfs in the  $(B - V, V - K)$  two-color diagram are well reproduced by pure hydrogen models down to  $T_{\text{eff}} \sim 5000$  K, below which the observed sequence seems to be better reproduced by the pure helium models (see their Fig. 9). A closer examination of the fits to the energy distributions of the cooler DA stars revealed that a missing opacity source near the  $B$  filter, resulting in an excess of flux in this region, was responsible for this discrepancy. When only wavelengths longward of  $B$  were considered, such as in  $(V - I, V - K)$  diagrams (see Fig. 13 of Bergeron et al. 1997 and Fig. 9 of Bergeron et al. 2001), the pure hydrogen models followed perfectly the observed DA sequence. For this reason, the  $B$  magnitude was excluded in the fits of the hydrogen-rich stars cooler than  $T_{\text{eff}} \sim 5500$  K.

Bergeron et al. (1997) proposed that this missing opacity source in the pure hydrogen models could be due to the bound-free opacity associated with the so-called dissolved atomic levels of the hydrogen atom, or pseudo-continuum opacity. When an electron makes a bound-bound transition from a lower level to an upper level, there is a finite probability that this upper level will be sufficiently perturbed by surrounding particles (a *dissolved* level) such that the electron is no longer bound to the nucleus, leading instead to a bound-free transition. This pseudo-continuum opacity can be treated within the Hummer-Mihalas formalism following the work of Hummer & Mihalas (1988) and Däppen et al. (1987), which we briefly describe for completeness.

The contribution of level  $i$  to the total monochromatic opacity is given in LTE by

$$\chi_i(\nu) = N_i \left[ \sum_{j>i} \frac{w_j}{w_i} \alpha_{ij}(\nu) + D_i(\nu) \alpha_{i\kappa}(\nu) \right] (1 - e^{-h\nu/kT}), \quad (1)$$

where the first term corresponds to the bound-bound opacities weighted by the occupation probability of each level of the transition. The occupation probability  $w_i$  of the atomic level  $i$  corresponds to the probability that an electron in this particular state is bound to the atom relative to a similar atomic state in a non-interacting environment. Correspondingly,  $(1 - w_i)$  is the probability that this state belongs to the continuum due to interactions with neighboring charged and neutral particles — the so-called dissolved levels.

The second term in equation (1) corresponds to the pseudo-continuum opacity, where  $\alpha_{i\kappa}(\nu)$  is the photoionization cross-section from level  $i$ , and  $D_i(\nu)$  is the *dissolved fraction* of levels given by the expression

$$D_i(\nu) = \frac{w_i - w_{n^*}}{w_i}, \quad (2)$$

where  $n^*$  corresponds to the effective quantum number of the atomic level reached after the absorption of a photon of energy  $h\nu$ , i.e.,

$$n^* = \left( \frac{1}{n_i^2} - \frac{h\nu}{\chi_H^I} \right)^{-\frac{1}{2}}. \quad (3)$$

The atomic level  $n^*$  is of course fictitious unless  $n^*$  has an integer value. An occupation probability  $w_{n^*}$  is assigned to that fictitious level by interpolating the value from the occupation probability of the real atomic levels. When  $n^*$  is negative ( $\nu > \chi_H^I/hn_i^2$ ), we define  $w_{n^*} \equiv 0$  (i.e.,  $D_i(\nu) = 1$ ), and the transition becomes a true bound-free transition. For positive values of  $n^*$ ,  $D_i(\nu)$  decreases with increasing wavelength, and the product of this term with the photoionization cross-section  $\alpha_{i\kappa}(\nu)$  — which is simply extrapolated below the frequency threshold — yields a pseudo-continuum opacity that gradually fades away from the unperturbed bound-free threshold. The pseudo-continuum opacity for the Balmer jump in typical white dwarf atmosphere conditions is illustrated in Figures 9 and 10 of Bergeron et al. (1991).

A problem arises if one considers the pseudo-continuum opacity originating from the Lyman edge. For instance, near 4000 Å, the dissolved fraction at the photosphere of a cool ( $T_{\text{eff}} \sim 4500$  K), hydrogen-rich white dwarf is typically  $10^{-4}$ . That is, electrons in the ground level of hydrogen making a corresponding transition to the fictitious level  $n^* \sim 1.14$  (setting  $n_i = 1$  and  $\lambda = 4000$  Å in equation [3]) have only a small 0.01% probability of going into the continuum, and to contribute to the bound-free opacity. However, since the pseudo-continuum opacity also depends on the population of hydrogen in the ground state, which is typically  $10^{20}\text{cm}^{-3}$  under such conditions, it remains the dominant opacity source, even in the infrared!

The problem is illustrated more quantitatively in Figure 4 where the contributions of the most relevant sources of opacity in a cool hydrogen-rich atmosphere are shown. The pseudo-continuum opacity from the  $n = 2$  level shows the expected behavior: the bound-free cross section with an unperturbed threshold at 3644 Å is extended towards longer wavelength, and is gradually attenuated by the dissolved fraction factor (see also Fig. 2 of Däppen et al. 1987). The behavior shown by the pseudo-continuum opacity from the  $n = 1$  level (dotted line) is obviously unphysical, however. The results would imply that this continuum opacity dominate all other sources of opacity at all wavelengths! This is a familiar problem for those who have attempted to implement the occupation probability formalism of Hummer-Mihalas in white dwarfs cooler than  $T_{\text{eff}} \sim 17,000$  K, where most of the hydrogen lies in the ground state. To overcome this problem, an arbitrary cutoff is usually applied, or the pseudo-continuum opacity from the Lyman edge is omitted altogether.

The exact reason why the Hummer-Mihalas formalism breaks down in this particular situation is not known, and a detailed analysis of this problem is outside the scope of this paper. We simply mention, as discussed in Bergeron et al. (1997), that far away from the Lyman jump, the calculation of the fraction of dissolved levels is probably unreliable. Indeed,  $D_i(\nu)$  is proportional to the difference between the occupation probability of the ground level and that of the upper (fictitious) dissolved level which, away from the edge, is located slightly above the ground level. As such,  $D(\nu)$  only *approaches* zero and its exact value is meaningless, and so is the value of the



corresponding pseudo-continuum opacity. The fact nevertheless remains that some form of pseudo-continuum opacity from the Lyman edge must exist in nature. This led Bergeron et al. (1997) to suggest that perhaps this neglected opacity could be responsible for the observed discrepancy at the blue end of the energy distribution of cool hydrogen-rich white dwarfs. After all, the ratio of the threshold opacity for the  $n = 1$  level is more than 9 orders of magnitude larger than that of the  $n = 2$  level, and it is not too farfetched to expect some of this pseudo-continuum opacity to affect the optical regions of the energy distribution.

Despite the lack of an accurate theory for calculating the fraction of dissolved levels far away from the Lyman edge, we may still make a suitable approximation by including a “damping” function into the pseudo-continuum opacity. Here we apply a damping function of the form

$$D_i(\nu)' = D_i(\nu) \exp\left(-\frac{\Delta\lambda}{\Delta\lambda_D}\right)^a, \quad (4)$$

where  $a$  and  $\Delta\lambda_D$  are arbitrary damping factors that remain to be determined. The results of the calculations with  $a = 1$  and  $\Delta\lambda_D = 350 \text{ \AA}$  are shown in Figure 4. This particular choice remains of course completely arbitrary but includes the two desired features, i.e. sufficient damping so that the overall energy distribution is still dominated by  $\text{H}^-$  in the optical and by  $\text{H}_2$  CIA in the infrared (not seen in Fig. 4), and not too much damping so that the pseudo-continuum opacity contributes to the total opacity near the blue end of the optical region.

## 6. Alternate Solution for WD 0346+246

Energy distributions calculated with this modified pseudo-continuum opacity are shown in Figure 5 for two cool white dwarfs taken from the analysis of Bergeron et al. (2001, note that for this comparison, the opacity has been included only in the calculation of the emergent fluxes but not in the model structure itself). LP 380–5 (WD 1345+238) is a DA white dwarf cooler than the temperature threshold at  $T_{\text{eff}} = 5500 \text{ K}$  below which the observed  $B$  magnitude of hydrogen-rich white dwarfs in the studies of Bergeron et al. (1997, 2001) is not well reproduced by the pure hydrogen models. The mismatch at  $B$  for this object is also illustrated in Figure 24 of Bergeron et al. (1997). LHS 2522 (WD 1208+576) is another DA star with a temperature slightly above this 5500 K threshold, and for which the fit at  $B$  is excellent. For LHS 2522, the inclusion of the pseudo-continuum opacity from the Lyman edge has reduced the theoretical fluxes for wavelengths shorter than the  $B$  bandpass, and the fit to the energy distribution is thus not affected by this additional opacity. For LP 380–5, however, the flux is considerably reduced near the  $B$  bandpass, and models that include the pseudo-continuum opacity reproduce the observed  $B$  magnitude quite well, as opposed to the model fluxes where this opacity is neglected.

Models were also calculated for mixed hydrogen and helium compositions in the temperature range of WD 0346+246. The pseudo-continuum opacity is more important in this object than in the

other two DA white dwarfs discussed above, not only because of its lower effective temperature, but mainly because of the increased atmospheric pressure resulting from the presence of helium. For this particular experiment, it was thus necessary to include self-consistently the pseudo-continuum opacity in the calculations of the model structures. In contrast with our previous fit, we now consider  $T_{\text{eff}}$ ,  $\log g$ , and  $N(\text{He})/N(\text{H})$  free parameters.

Our best fit for WD 0346+246 is shown in the top panel of Figure 5. Also shown for comparison is the optical and infrared spectra from Oppenheimer et al. (2001b, note that the fluxes from the optical spectrum have been multiplied here by a factor of 1.08 in order to match with the observed photometry). The results indicate that a good fit to the energy distribution of WD 0346+246 can be achieved with a temperature of  $T_{\text{eff}} = 3830$  K, close to the previous solution at  $T_{\text{eff}} = 3750$  K, but with a helium-to-hydrogen abundance ratio close to unity. In particular, the fit at  $B$  and  $V$  is greatly improved by the inclusion of the pseudo-continuum opacity, with respect to the fit obtained when this opacity is neglected. Our fit can also be contrasted with that shown in Figure 15 of Fontaine et al. (2001) for the same object, based on slightly different photometric observations, and where the  $B$  and  $V$  magnitudes were simply omitted from the fit because of the suspected missing opacity in this region.

A more careful examination of the results shown in Figure 5 also reveals that even though the inclusion of a pseudo-continuum opacity from the Lyman edge provides an overall good fit to the observed energy distribution of WD 0346+246, our approximate treatment could still be improved. If we take the observed spectrum at face value, the pseudo-continuum opacity seems to extend at much longer wavelengths, and to have the wrong frequency dependency. As an illustrative example, by using different factors  $a = 0.52$  and  $\Delta\lambda_{\text{D}} = 36 \text{ \AA}$  in equation (4), and by repeating the complete fitting procedure described above, we obtain the fit shown in Figure 6. The atmospheric parameters obtained with this modified damping function —  $T_{\text{eff}} = 3780$  K,  $\log g = 8.34$ ,  $N(\text{He})/N(\text{H}) = 1.3$  — are comparable to those given in Figure 5, but the resulting fit is significantly better. In particular, the slope and extent of the pseudo-continuum opacity are reproduced much better. The pseudo-continuum opacity profile at the photosphere of the corresponding model atmosphere is shown in the bottom panel of Figure 6 together with the other most relevant opacity sources.

We also note that the surface gravity inferred from our best fit has been constrained from the measured trigonometric parallax  $\pi = 36 \pm 5$  mas (Hambly et al. 1999), which implies a radius of  $R = 0.0100 R_{\odot}$  and a mass of  $M = 0.80 M_{\odot}$ . In contrast, the former solution shown in Figure 2 as well as that of Oppenheimer et al. (2001b) both *assumed*  $\log g = 8.0$ , which yields a radius of  $R = 0.01256 R_{\odot}$  and a distance of  $D = 35.5$  pc, inconsistent with the measured distance of  $D = 27.8$  pc. Using the evolutionary models discussed in Bergeron et al. (2001) with C/O cores, helium envelopes of  $q(\text{He}) = 10^{-2}$ , and “thick” outermost hydrogen layers of  $q(\text{H}) = 10^{-4}$ , we derive an age for WD 0346+246 of  $\tau = 11.0$  Gyr; “thin” layer models with  $q(\text{H}) = 10^{-10}$  yield  $\tau = 8.7$  Gyr.

As discussed in § 4, the extreme helium-rich composition proposed by Oppenheimer et al.

(2001b) for WD 0346+246 implies accretion rates from the interstellar medium that are unrealistically small. Adopting instead  $N(\text{He})/N(\text{H}) = 1$  as our best estimate, we derive a total hydrogen mass of  $2 \times 10^{-7} M_{\odot}$ . If WD 0346+246 has evolved from an almost pure helium atmosphere — i.e. a DB star, the total amount of hydrogen accreted corresponds to a time-averaged accretion rate of  $\sim 2 \times 10^{-17} M_{\odot} \text{ yr}^{-1}$ , in good agreement with the theoretical estimates of Wesemael (1979) and Dupuis et al. (1993). Alternatively, WD 0346+246 may have evolved from a thin hydrogen layer DA star that has been convectively mixed below  $T_{\text{eff}} \sim 12,000$  K. According to Figure 40 of Bergeron et al. (1997), the minimum helium-to-hydrogen abundance ratio that can be achieved for a  $0.8 M_{\odot}$  white dwarf is when the hydrogen atmosphere with a mass of  $M(\text{H}) \sim 2.5 \times 10^{-8} M_{\odot}$  is convectively mixed at  $T_{\text{eff}} \sim 5000$  K. This yields an abundance of  $N(\text{He})/N(\text{H}) \sim 8$ . Hence, to arrive at an abundance of  $N(\text{He})/N(\text{H}) = 1$  by the time the star has cooled down to  $T_{\text{eff}} = 3800$  K, it must accrete an extra  $\sim 1.8 \times 10^{-7} M_{\odot}$  of hydrogen over a period of  $\sim 1.6$  Gyr (assuming here thin hydrogen models), which corresponds to an accretion rate of  $\sim 10^{-17} M_{\odot} \text{ yr}^{-1}$ . Hence it is not possible from these arguments alone to determine whether WD 0346+246 has evolved from a thin hydrogen-layer DA white dwarf, or from a hot DB star.

We also discussed the fact that the extreme helium-rich composition solution for WD 0346+246 was unlikely because of the effects the presence of even small amounts of elements heavier than helium have on the predicted fluxes (see Fig. 3). Our solutions presented in Figures 5 or 6 are not sensitive to the presence of these additional elements since hydrogen remains the most important contributor of free electrons. Additional calculations not shown here indicate that the emergent fluxes are not affected even when the calcium abundance is set to a value as high as  $N(\text{Ca})/N(\text{He}) = 10^{-8}$ . Our solution is thus robust against the presence of such additional elements.

## 7. Conclusions

In this paper we have reexamined the atmospheric parameters of the halo white dwarf WD 0346+246. A solution at  $T_{\text{eff}} \sim 3750$  K with an extremely low hydrogen abundance has been found,  $N(\text{H})/N(\text{He}) = 10^{-9}$ , in agreement with the conclusions of Oppenheimer et al. (2001b). We have showed, however, that such a low hydrogen content is very unlikely due to accretion from the interstellar medium over a cooling age of roughly 10 Gyr. Furthermore, this solution was shown to be extremely volatile when even minute amounts of heavy elements were included in the atmosphere. We have proposed instead a solution where hydrogen and helium are present in the atmosphere of WD 0346+246 in nearly equal amounts. A good fit has been achieved by including a pseudo-continuum opacity originating from the dissolved levels of hydrogen. This opacity has been parameterized with an *ad hoc* damping function, however, and it is clear that a better physical description must be sought before more quantitative results can be achieved.

The presence of this missing opacity source had already been foreseen in the study of cool hydrogen-rich white dwarfs by Bergeron et al. (1997, 2001) who refrained from interpreting two-color diagrams where one of the filters may be affected by this missing opacity, no matter what

its origin might be —  $(B - V, V - K)$  diagrams for instance. These studies have also shown that for the coolest ( $T_{\text{eff}} \sim 4000$  K) hydrogen-rich stars, even the  $V$  filter may be affected. The results presented in this paper also support this conclusion (see Fig. 5). It thus appears extremely dangerous to interpret these newly discovered ultracool white dwarfs in two-color or color magnitude diagrams which involve “blue” magnitudes (see, e.g., Harris et al. 1999, 2001; Oppenheimer et al. 2001a,b) until this problem with the missing opacity has been properly dealt with, and included in the theoretical models and colors.

It now remains to be seen whether this new opacity source, even when included with the approximate treatment introduced in this paper, can help resolve the mystery surrounding several ultracool white dwarfs whose energy distributions have yet failed to be successfully explained in terms of hydrogen or mixed hydrogen/helium compositions.

We are grateful to S. T. Hodgkin for providing us with the spectrum of WD 0346+246, and to G. Fontaine and F. Wesemael for a careful reading of the manuscript. This work was supported in part by the NSERC Canada and by the Fund FCAR (Québec).

## REFERENCES

- Bergeron, P., Leggett, S. K., & Ruiz, M. T. 2001, *ApJS*, 133, 413
- Bergeron, P., Ruiz, M. T., & Leggett, S. K. 1997, *ApJS*, 108, 339
- Bergeron, P., Ruiz, M. T., Leggett, S. K., Saumon, D., & Wesemael, F. 1994, *ApJ*, 423, 456
- Bergeron, P., Saumon, D., & Wesemael, F. 1995, *ApJ*, 443, 764
- Bergeron, P., Wesemael, F., & Fontaine, G. 1991, *ApJ*, 367, 253
- Däppen, W., Anderson, L., & Mihalas, D. 1987, *ApJ*, 319, 195
- Dupuis, J., Fontaine, G., Pelletier, C., & Wesemael, F. 1992, *ApJS*, 82, 505
- Dupuis, J., Fontaine, G., & Wesemael, F. 1993, *ApJS*, 87, 345
- Fontaine, G., Brassard, P., & Bergeron, P. 2001, *PASP*, 113, 409
- Hambly, N. C., Smartt, S. J., & Hodgkin, S. T. 1997, *ApJ*, 489, L157
- Hambly, N. C., Smartt, S. J., Hodgkin, S. T., Jameson, R. F., Kemp, S. N., Rolleston, W. R. J., & Steele I. A. 1999, *MNRAS*, 309, L33
- Hansen, B. M. S. 1998, *Nature*, 394, 860
- Harris, H. C., Dahn, C. C., Vrba, F. J., Henden, A. A., Liebert, J., Schmidt, G. D., & Reid, I. N. 1999, *ApJ*, 524, 1000
- Harris, H. C., et al. 2001, *ApJ*, 549, L109
- Hummer, D. G., & Mihalas, D. 1988, *ApJ*, 331, 794
- Ibata, R., Irwin, M., Bienaymé, O., Scholz, R., & Guibert, J. 2000, *ApJ*, 532, L41
- Jørgensen, U. G., Hammer, D., Borysow, A., & Falkesgaard, J. 2000, *A&A*, 361, 283
- Knox, R. A., Hawkins, M. R. S., & Hambly, N. C. 1999, *MNRAS*, 306, 736
- Lenzuni, P., Chernoff, D. F., & Salpeter, E. E. 1991, *ApJS*, 76, 759
- Liebert, J., Dahn, C. C., & Monet, D. G. 1988, *ApJ*, 332, 891
- Malo, A., Wesemael, F., & Bergeron P. 1999, *ApJ*, 517, 901
- Monet, D. G., Dahn, C. C., Vrba, F. J., Harris, H. C., Pier, J. R., Luginbuhl, C. B., & Ables, H. D. 1992, *AJ*, 103, 638

- Oppenheimer, B. R., Hambly, N. C., Digby, A. P., Hodgkin, S. T., & Saumon, D. 2001a, *Science*, in press
- Oppenheimer, B. R., Saumon, D., Hodgkin, S. T., Jameson, R. F., Hambly, N. C., Chabrier, G., Filipenko, A. V., Coil, A. L., & Brown, M. E. 2001b, *ApJ*, 550, 448
- Reid, I. N., Sahu, K. C., & Hawley, S. L. 2001, *ApJ*, submitted
- Saumon, D., & Jacobson, S. B. 1999, *ApJ*, 511, L107
- Tassoul, M., Fontaine, G., & Winget, D. E. 1990, *ApJS*, 72, 335
- Wesemael, F. 1979, *A&A*, 72, 104
- Zeidler-K. T., E.-M., Weidemann, V., & Koester, D. 1986, *A&A*, 155, 356

Fig. 1.— Energy distribution of white dwarf model atmospheres with  $T_{\text{eff}} = 3750$  K,  $\log g = 8.0$ , and various helium-to-hydrogen abundance ratios. All distributions are normalized to unity where the Eddington flux ( $H_\nu$ ) is maximum. The thick solid and dashed lines represent respectively the pure hydrogen and pure helium atmospheric compositions. The thin solid lines correspond to (starting from the pure hydrogen model)  $N(\text{He})/N(\text{H}) = 0.1, 1, 10$ , and  $10^5$ , while the thin dashed lines correspond to (starting from the  $N(\text{He})/N(\text{H}) = 10^5$  model)  $N(\text{He})/N(\text{H}) = 10^8, 10^{10}, 10^{12}$ , and  $10^{13}$ .

Fig. 2.— Our best fit to the energy distribution of WD 0346+246 in terms of  $\log f_\lambda$  (top panel) and  $f_\nu$  (bottom panel);  $T_{\text{eff}}$  and  $\log g$  are taken from Oppenheimer et al. (2001b). The *BVRI* and *JHK* photometric observations are represented by error bars. The solid lines represent the model monochromatic fluxes, while the filled circles correspond to the model fluxes averaged over the filter bandpasses.

Fig. 3.— Energy distribution of white dwarf model atmospheres with  $T_{\text{eff}} = 3750$  K,  $\log g = 8.0$ ,  $\log N(\text{He})/N(\text{H}) = 9.1$ , and for various calcium-to-helium abundance ratios. All distributions are normalized to unity where the Eddington flux ( $H_\nu$ ) is maximum. The various models correspond to (starting from the thick line)  $N(\text{Ca})/N(\text{He}) = 0, 10^{-14}, 10^{-13}$ , and  $10^{-12}$ . The observed photometry of WD 0346+246, normalized with the scaling factor determined from the zero-metal solution (see Fig. 2), is represented by error bars.

Fig. 4.— Most relevant sources of opacity at the photosphere ( $\tau_{\text{R}} = 1$ ) of a pure hydrogen model atmosphere at  $T_{\text{eff}} = 4600$  K and  $\log g = 7.75$  (the atmospheric parameters of LP 380–5 shown in Fig. 5). The local temperature and density are indicated in the figure, and each opacity source is identified as well. The thick solid line represents the total opacity. The bound-free opacities from the  $n = 1$  and  $n = 2$  levels include the pseudo-continuum opacity from the dissolved levels, while the contributions from the unperturbed bound-free absorptions alone are represented by the dashed lines. The pseudo-continuum opacity from the  $n = 1$  level calculated explicitly by equations (1) to (3) is shown as a dotted line, and that calculated with the damping function given by equation (4) with  $a = 1.0$  and  $\Delta\lambda_{\text{D}} = 350$  Å is shown by the solid line.

Fig. 5.— Our best fit to the energy distribution of WD 0346+246, as well as fits to LHS 2522 and LP 380–5 taken from Bergeron et al. (2001). The *BVRI* and *JHK* photometric observations are represented by error bars. The solid and dotted lines represent respectively the model fluxes with and without the pseudo-continuum opacity from the Lyman edge, while the filled circles correspond to the model fluxes — with the pseudo-continuum opacity included — averaged over the filter bandpasses. The upper panel also shows for comparison the optical and infrared spectra from Oppenheimer et al. (2001b).

Fig. 6.— *Top panel:* Our best fit to the energy distribution of WD 0346+246 using a pseudo-continuum opacity calculated with the damping function given by equation (4) with  $a = 0.52$  and  $\Delta\lambda_{\text{D}} = 36$  Å. *Bottom panel:* Most important sources of opacity at the photosphere ( $\tau_{\text{R}} = 1$ ) of the

corresponding model atmosphere. The local temperature and density are indicated in the figure, and each opacity source is identified as well. The thick solid line represents the total opacity. The bound-free opacity from the  $n = 1$  level includes the pseudo-continuum opacity from the dissolved levels, while the contribution from the unperturbed bound-free absorptions alone is represented by the dashed line. The feature near  $0.05 \mu m$  is the ionization threshold from neutral helium.



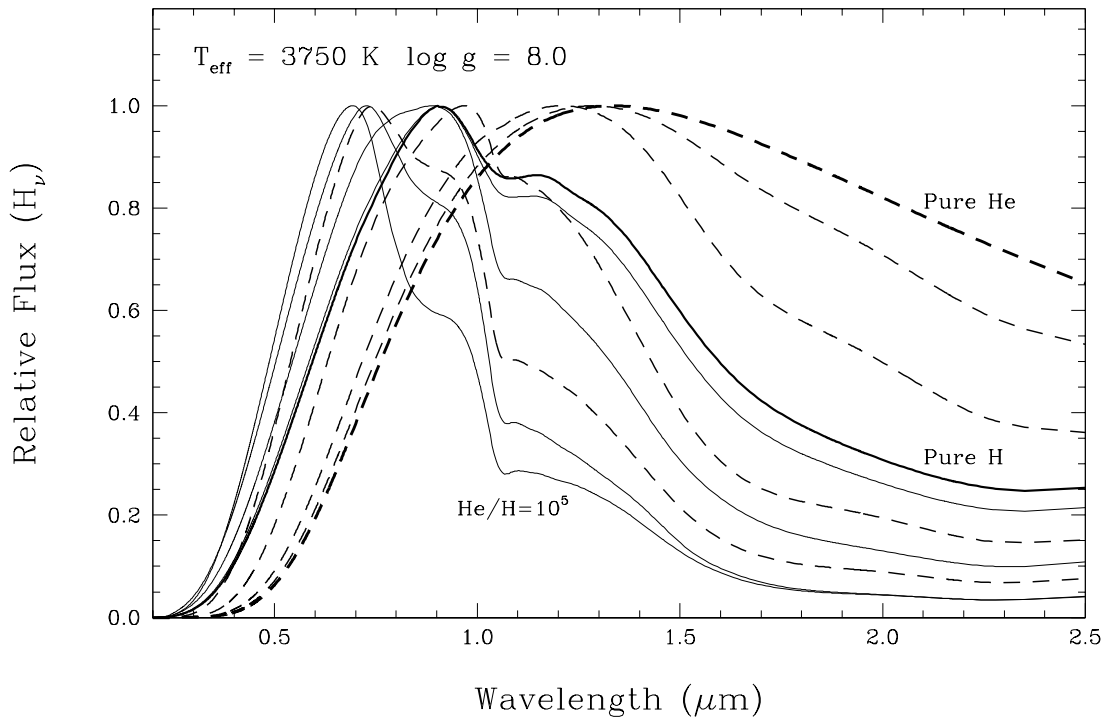


Figure 1

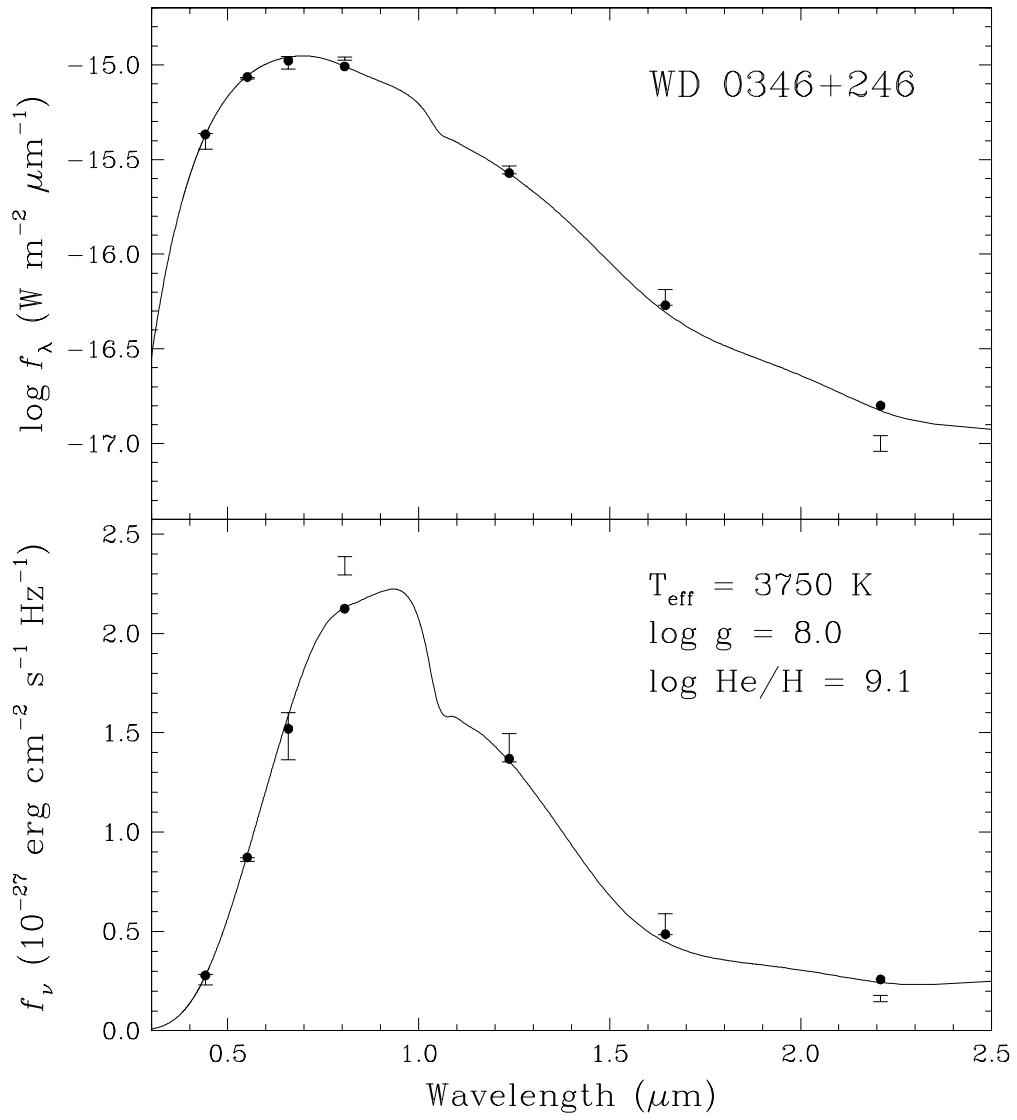


Figure 2

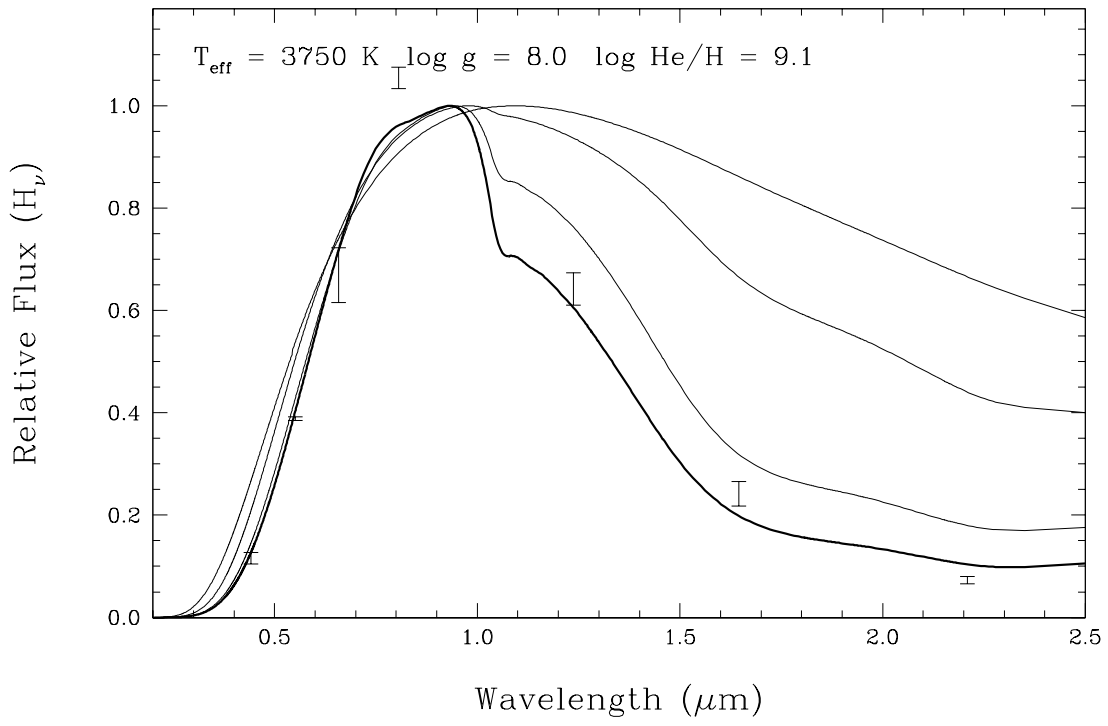


Figure 3

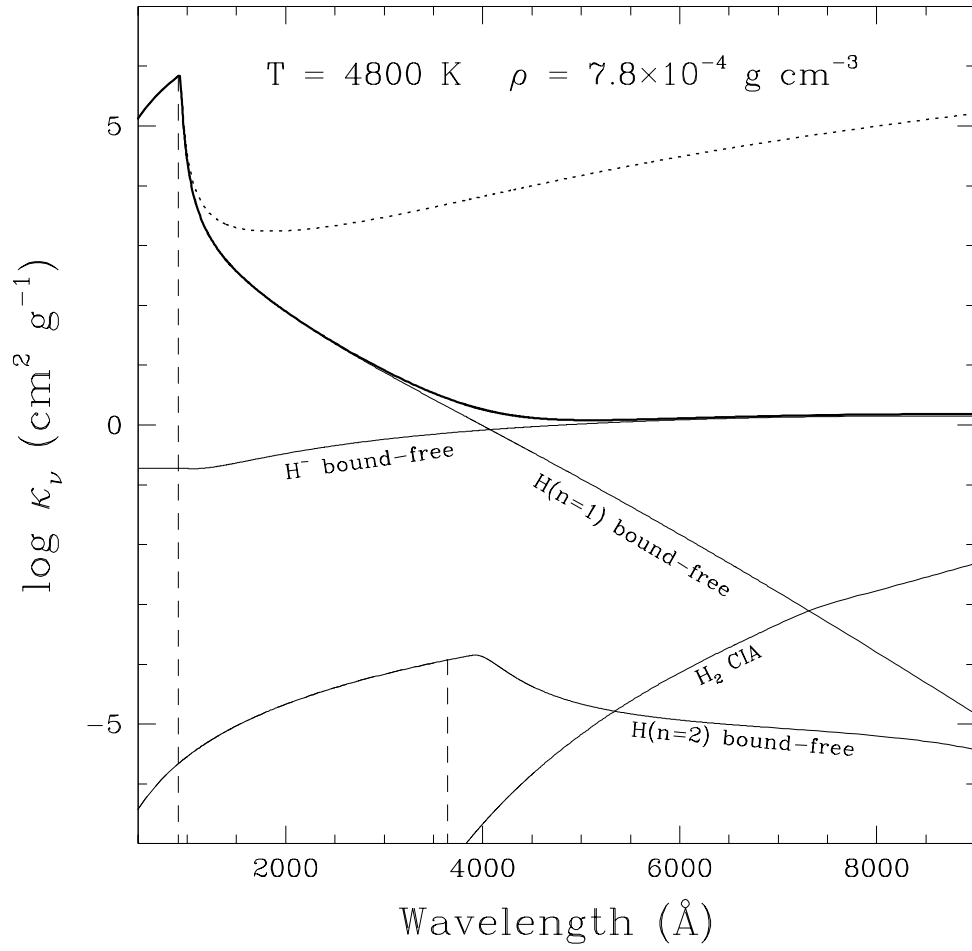


Figure 4

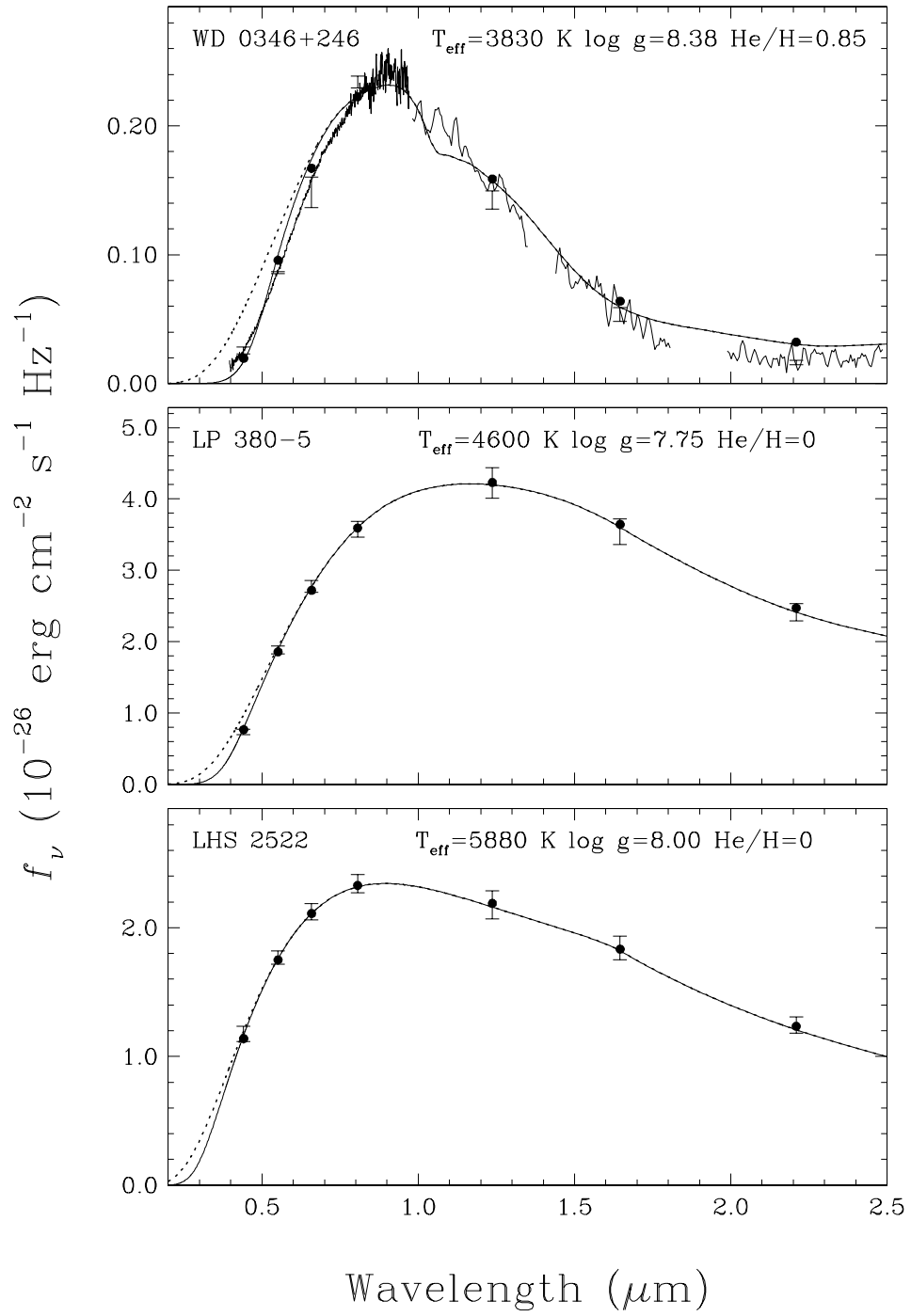


Figure 5

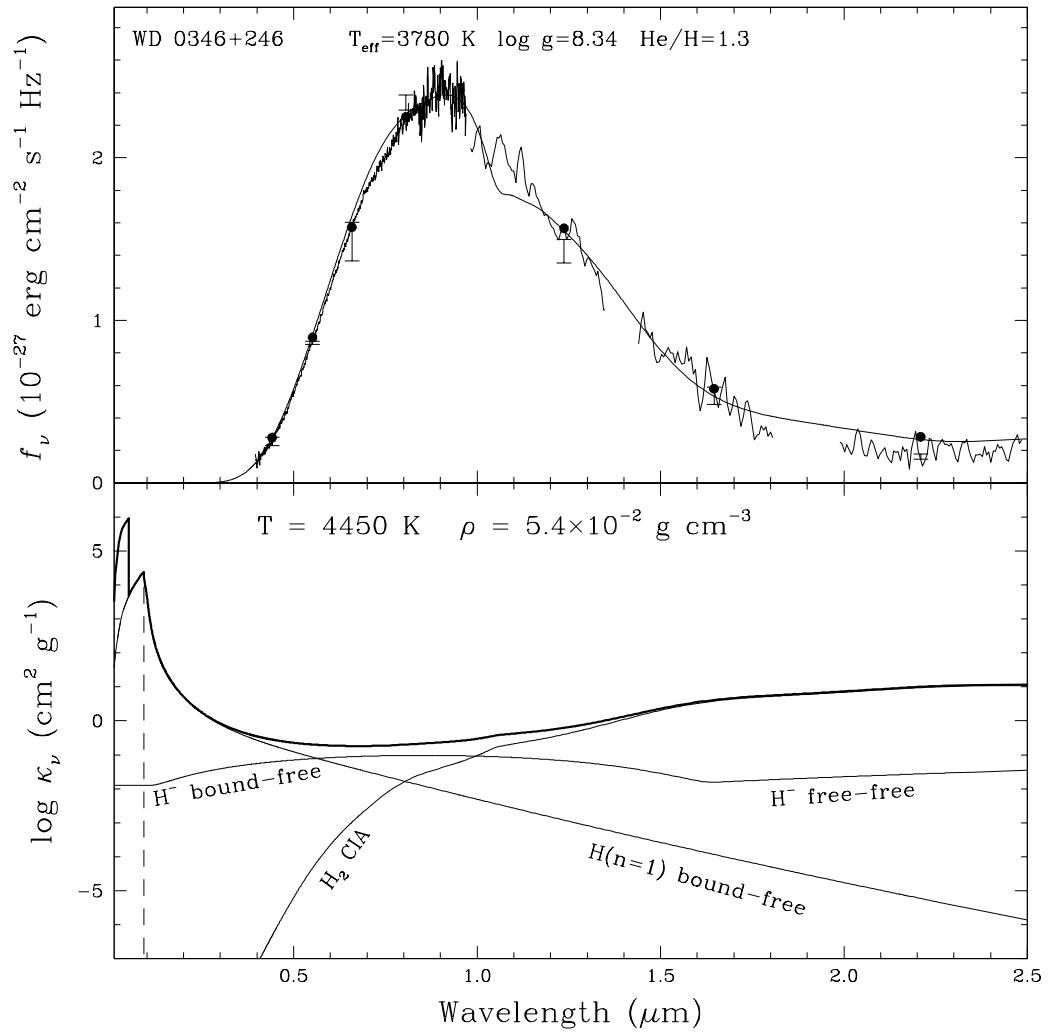


Figure 6